Available online at www.sciencedirect.com
SCIENCE DIRECT®
Journal of Power Sources 123 (2003) 172–181
JOURNAL OF POWER SOURCES
www.elsevier.com/locate/jpowsour

Novel microfabrication approaches for directly patterning PEM fuel cell membranes

Keyur Shah*, W.C. Shin, R.S. Besser

Department of Chemical, Biochemical and Materials Engineering, Stevens Institute of Technology, Castle Point on Hudson, Hoboken, NJ 07030, USA

Received 8 March 2003; accepted 31 March 2003

Abstract

We have successfully developed miniature hydrogen-air proton exchange membrane (PEM) fuel cells (FC) on silicon and polydimethylsiloxane (PDMS) base substrates using conventional and non-conventional microfabrication technologies. Prototype base substrates were fabricated by using well-known micromachining technologies, such as photolithography, deep reactive ion etching, and soft lithography. Sputtering, a physical vapor deposition method, was used to deposit catalysts and electrodes directly on the surface of the Nafion PEM. This paper describes the novel microfabrication approaches employed to selectively deposit electrodes and catalyst materials on the membrane with improved morphology and structure of electrodes. The aim was to reduce precious metal catalyst loadings, ohmic (*iR*) losses, and to improve structural support for the thin-film FC with concurrent reduction in fabrication complexity.

Keywords: Miniature power; Microfabrication techniques; Vacuum sputtering; Microreactor; PDMS; Nafion membrane

1. Introduction

As fuel cells (FC) rapidly mature, they are gaining more attention as clean and energy efficient power sources, with growing importance for preserving the environment as they produce environmentally benign energy [1]. Among the wide variety of areas in which fuel cells can be employed, one of the promising fields of applications is their use as portable power sources making them prominent alternatives to batteries as miniature, lightweight power sources [1,2]. Micro proton exchange membrane (PEM) fuel cells, because of their ability to deliver higher energy per volume and weight, can meet the demands of advanced portable electronic devices and can be directly integrated and used as onboard power sources in the sub-Watt range to operate small sensors and actuators. At slightly higher output powers, they can be used in other applications to power portable electronic devices like cell phones (∼1 W), laptop computers (∼20 W), etc. [3].

The current approach to developing miniature fuel cells is based on adoption of micromachining technologies. The use of silicon micromachining and related thin film processes have been employed by several research groups as an attractive route for fabrication [4–9]. These techniques enable simple stacking of fuel cell components on a chip for compact, lightweight, scalable power generation.

We developed the miniature fuel cell with a dual purpose. First, it can be used as a portable power source as described above. As a second application, it can be used as a simple and flexible development tool to explore fuel cell materials and components. A number of technical issues such as cost, performance, materials, etc., need to be resolved to commercialize fuel cells [10], hence, extensive research efforts are necessary in order to develop novel, cheap, fuel cell materials, to reduce electrocatalyst loadings, and to simplify manufacturing processes. These microstructures enable rapid fabrication and testing of compact laboratory fuel cells with a variety of material transfer options to develop and screen the cell materials with little infrastructure requirements and also allow testing in explosion-free conditions. These miniature fuel cells have the potential to be fast, reliable, safe, economical, and environmentally friendly test structures to study and develop novel fuel cell manufacturing processes and materials.

2. Micro fuel cell design

Miniature fuel cells demand an extremely simple and compact design in order to be useful as portable power sources. The aim was to make a simple functioning device

* Corresponding author. Tel.: +1-201-216-5332; fax: +1-201-216-8306.
E-mail address: kshah5@stevens-tech.edu (K. Shah).

0378-7753/$ – see front matter © 2003 Published by Elsevier B.V.
doi:10.1016/S0378-7753(03)00538-X

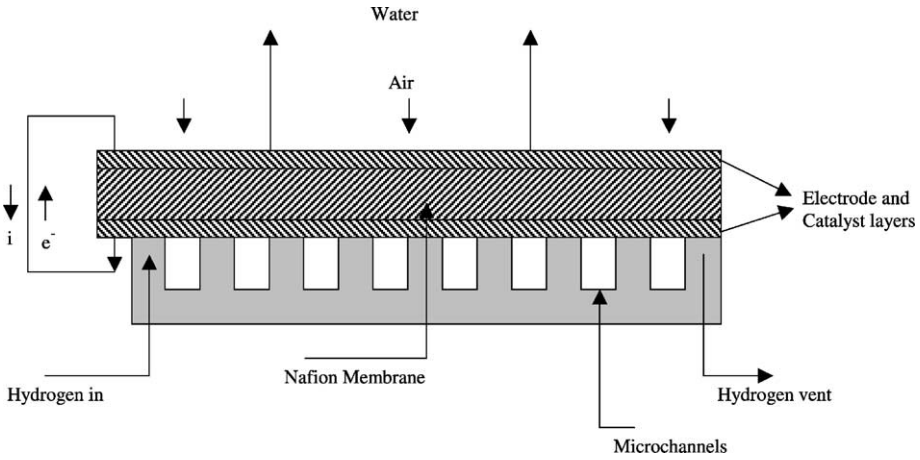

Fig. 1. Schematic of a micro proton exchange membrane fuel cell.

on a silicon substrate by adapting the design of a conventional proton exchange membrane fuel cell. Fig. 1 shows the schematic of a micro PEM fuel cell.

The device consists of a base substrate with microchannels (based on an existing design of a silicon microreactor we used in previous experiments) to introduce and distribute gaseous fuel, the anode and cathode electrodes, the proton conducting membrane, and the external electric circuit. We employed silicon and poly-dimethylsiloxane (PDMS) as base substrates and their associated fabrication techniques to create flow structures. A thin solid sheet of Nafion membrane was used as the electrolyte. Electrodes and catalysts were selectively deposited as anode and cathode on both sides of this membrane using vacuum sputtering. This membrane was then bonded to the base substrate such that the anode side faced the flow channels. The membrane was extended from the base on one edge so that it remained free standing to provide electrical connections to both sides. The cathode side was kept open to draw oxygen from the ambient air.

Hydrogen enters through the inlet via of the base substrate and distributes along the microchannels. The hydrogen then reacts in the presence of the catalyst to form protons and electrons. Electrons conduct through the external circuit producing electrical current and reach the cathode, while protons pass through the Nafion membrane from anode to cathode, where they react with oxygen in the presence of electrons to form water, which is allowed to vaporize into the ambient.

3. Experimental

3.1. Fabrication of silicon and PDMS microreactors

We have successfully employed microfabrication techniques for microreactor fabrication using well-characterized processes [11–14]. These processes employed bulk micromachining techniques, which essentially remove the silicon from its bulk to form structures on the silicon wafer. The microreactors were fabricated by employing a multi-step photolithography process using three separate masks. These included two front side masks for (a) inlet and outlet and (b) channels. The third mask was for a backside patterning of inlet and outlet vias.

The starting material was a 4 in. diameter, 550 μm thick double-side polished silicon wafer. The masks were designed to give eight microreactors on a single wafer. Positive photoresists were used to transfer patterns from chrome mask to silicon wafer. The resist was used as a mask for the subsequent silicon etching process instead of oxide because of ease of processing and lower cost, as it does not involve the extra step of removing oxide by wet etching methods. These patterns were then transferred into silicon by using the deep reactive ion etching process [14]. The fabricated wafer was sent outside for dicing (MPE Inc., Greenville, TX) into individual microreactors of size 3.1 cm × 1.6 cm. Fig. 2 shows a single diced silicon microreactor chip.

In order to reduce the overall cost of the fuel cell with a view toward commercialization, it is necessary to produce this cell on cheaper base substrates. We therefore explored the fabrication of PDMS microreactors as base substrates upon which the cell components were vertically stacked. PDMS microreactors were fabricated by employing micromolding, a soft lithography method [15]. The PDMS microreactors had the same design and consisted of inlet, outlet and channels that were cast against a microfabricated silicon master. The silicon master for soft lithography was fabricated using photolithography and dry etching processes. The same reactor masks were used as were described above for the fabrication of the silicon microreactor. However, since the fabricated master should have an inverse of the desired pattern, negative resist on a silicon wafer support was used in order to create the master. The liquid prepolymer of PDMS was then spin-coated on the master support wafer a number of times to get a total thickness of around 500 μm. The PDMS was cured and peeled-off from the master, which produced an exact replica of eight microreactors on a single

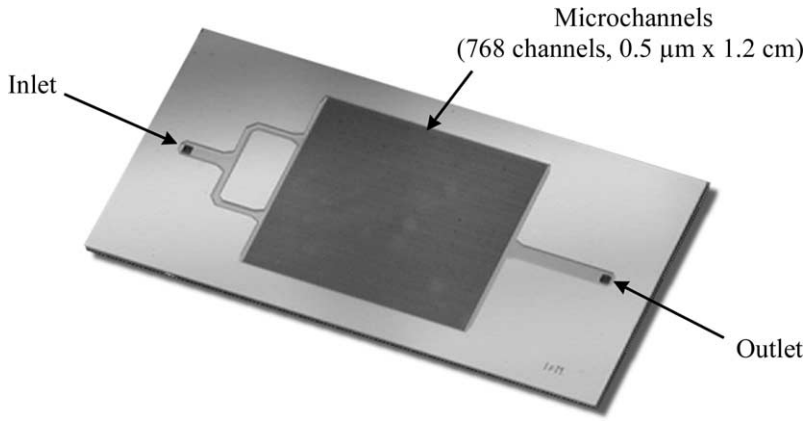

Fig. 2. Silicon base substrate with micro flow channels (microreactor) to introduce and distribute gaseous fuel.

PDMS membrane. Individual PDMS microreactors were then cut with a razor blade to the size of 3.1 cm × 1.6 cm. Fig. 3 shows a diced PDMS microreactor chip.

3.2. Selective deposition of electrodes and catalysts on Nafion membrane

The combination of anode/electrolyte/cathode in a PEMFC is referred to as the membrane electrode assembly (MEA) [2]. It is the key component of the PEMFC, since it is the site where the cell reactions take place. It consists of a solid membrane, with a layer of electrocatalyst and gas porous electrodes on both sides, forming the anode and cathode of the cell. The electrodes consist of catalyst particles, which are normally Pt, Pt alloys, or other noble metal alloys.

Traditionally, MEAs have been manufactured by attaching a catalyst layer on one side of porous gas diffusion electrodes. The catalyst layers can be deposited by means of painting, printing, and spraying inks that contain a mixture of electrolyte and carbon supported catalyst [16–19]. A primary role of the carbon support is to provide electrical connection between the widely dispersed Pt catalyst nanoclusters and the electrodes. To enhance transport of protons within the catalyst layer, Nafion may be mixed with the catalyst [17]. The gas diffusion electrodes serve as the electron collector and also facilitate permeation of the reactant gases. The gas diffusion electrodes typically consist of a cloth woven from carbon fibers [16]. The membrane is then hot pressed at an elevated temperature slightly above its glass transition temperature between these two electrodes in such a way that the catalyst layer faces the membrane side and the other side faces the flow field plates. In addition to Nafion impregnated with Pt/C, various electrode structures and catalyst layers have been employed, such as electrodeposited and sputter-deposited thin film of Pt in order to reduce the content of electrocatalyst in the electrode layers while maintaining cell performances [20,21].

A primary goal of our method of creating the MEA was greater simplicity of processing. We used vacuum sputtering to deposit catalysts and electrodes directly on the membrane surface. An US Gun II Planar Magnetron Sputtering machine was used for this purpose. Researchers have successfully employed sputter deposition techniques in order to achieve ultra-low levels of catalyst loadings [20–23], which in turn reduce the cell cost and result in better utilization of the catalyst. Sputtering can easily provide thin and uniform deposition on the membrane surface [24].

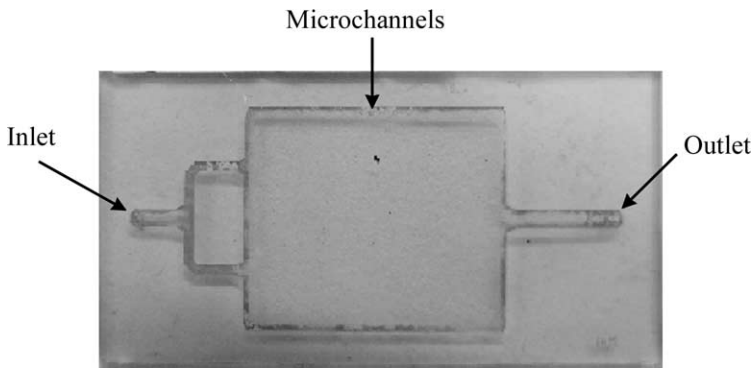

Fig. 3. PDMS base substrate with inlet, outlet and micro flow channels to introduce and distribute gaseous fuel in a fuel cell.

The proton exchange membrane was Dupont Nafion 112 (2 mil thickness) from Electrochem Inc. (Woburn, MA). The membrane was pretreated in various chemicals in order to remove organic and inorganic impurities. This procedure involved sequential immersion of the membrane in a boiling solution of 3 wt.% aqueous hydrogen peroxide (H_2O_2) solution for 1 h, DI water for 1 h, 0.5 M H_2SO_4 solution for 1 h, and DI water for 1 h. After pretreatment, the membrane was dried and sputtered using a shadow mask to define the catalyst layer on both sides of the membrane. The samples were removed from the vacuum chamber, flipped and then returned to the chamber to deposit the back side.

We found that the Nafion membrane dehydrated under vacuum, however it rehydrated quickly after being re-exposed to the ambient. Since the sputter deposition is under vacuum conditions, it was necessary to hold the membrane firmly on some base when it was placed in the vacuum chamber to avoid wrinkle formation, which would result in non-uniform deposits. The base used for the purpose was a PDMS-coated silicon wafer, as Nafion adheres well to PDMS. For this purpose, PDMS was spun onto a silicon wafer and allowed to cure. The Nafion membrane was cut into 4 in. size and placed on the same size PDMS-coated wafer.

We used a shadow mask made from a Mylar sheet to deposit thicknesses of 400 and 150 nm of platinum as the electrode and catalyst on both the sides of the membrane to define anode and cathode of the fuel cell. However, we found that the boundaries of deposited metals were not uniform with this hard mask. The contact between the rigid mask and the membrane was very poor, which led to non-uniform deposition due to the presence of an air gap between the mask and the membrane.

3.3. PDMS shadow masks for electrode and catalyst deposition on membrane

We found that the performance of platinum sputtered fuel cells showed strong dependence on the thickness of the catalyst layer. From experimental results with 400 and 150 nm thick platinum as combined electrode–catalyst, we realized that the performance could be improved by further reducing the thickness of catalyst layer. To reduce the catalyst loading further, it was necessary to use some other conductive materials as electrodes together with catalyst materials in order to reduce series and contact resistances. As a current collector, the electrode must provide a sufficiently open surface for reactant gas to diffuse in order to access the catalyst sites while minimizing series resistance effects that would lead to ohmic losses. This structure should also provide mechanical support to the membrane piece. Ag was chosen as the electrode material since it is highly conductive and easy to sputter. Sputtered Ag fuel cell electrodes have been successfully employed by researchers in the past [25,26].

In order to selectively deposit electrodes and catalyst layers on Nafion membranes, we employed an elastomeric shadow mask of PDMS. The technique of using PDMS elastomeric membranes as dry resists and for dry lift-off was reported earlier by Whiteside's group at Harvard University [27]. We found that PDMS seals well with the Nafion membrane, giving conformal contact with no air gap to provide well-defined boundaries of deposited metals. The PDMS shadow mask was fabricated by spin-coating liquid PDMS onto a silicon master, which consisted of photoresist structures defined by photolithography. The master was fabricated on a silicon wafer by either patterning with thick positive (AZ-100 XT) or negative (SU-8) photoresist to define posts on the wafer or by using thin photoresist followed by dry etching of the silicon to produce taller structures on the silicon wafer. PDMS was then spin-coated at an appropriate speed such that the height of the layer was lower than the height of the features on the master. After curing, the PDMS layer was peeled away from the master, and had openings in locations corresponding to the raised features on the master. These fabrication processes to obtain a PDMS shadow mask are shown in Fig. 4.

Two separate masks were designed for the fabrication of master wafers for producing the PDMS shadow masks for catalyst and electrode deposition. The masks were designed to give four separate patterns on a single 4 in. wafer. For the catalyst deposition mask, the patterned area was 1.4 cm × 1.2 cm, to correspond to the microchannel zone of the microreactor and 0.5 cm × 0.5 cm for the pad on the edge to provide electrical contacts. The electrode mask consisted of isolated circles and squares 100 μm in size and spacing placed within the entire channel zone.

The silicon masters were exposed before use to the vapor of (tridecafluoro-1,1,2,2,-tetrahydro-octyl)-1-trichlorosilane (Gelest Inc., Morrisville, PA) in a vacuum desiccator for easy peeling-off of the PDMS membrane. This treatment lowers the surface energy of the substrate to ease the removal of PDMS from the master [28]. A liquid prepolymer of PDMS was then spin-coated onto a master. The rate of spinning was adjusted so that the thickness of the PDMS layer was less than the height of the photoresist posts on the master wafer to prevent bridging of PDMS into what should be open areas. The PDMS was spin-coated at 1000 rpm for 60 s with acceleration of 300 revolutions/s to yield a 70 μm thick PDMS membrane. The PDMS was then cured at 100 °C for 2 h. After curing, to release the membrane, it was cut around the edges with a razor blade. The membrane was then peeled away from the master. Peeling-off the membrane from the master gave an array of holes in the PDMS allowing it to be used as a shadow mask for metal deposition on the Nafion membrane. Fig. 5 shows scanning electron micrograph (SEM) images of arrays of 100 μm squares and circular holes formed in the PDMS.

The pretreated Nafion membrane was cut to a 4 in. diameter piece and placed on the cured PDMS-coated support wafer. First, 5 nm of catalyst (Pt or Pd) was deposited on the Nafion membrane using the respective PDMS shadow mask, which formed a tight and conformal seal with the

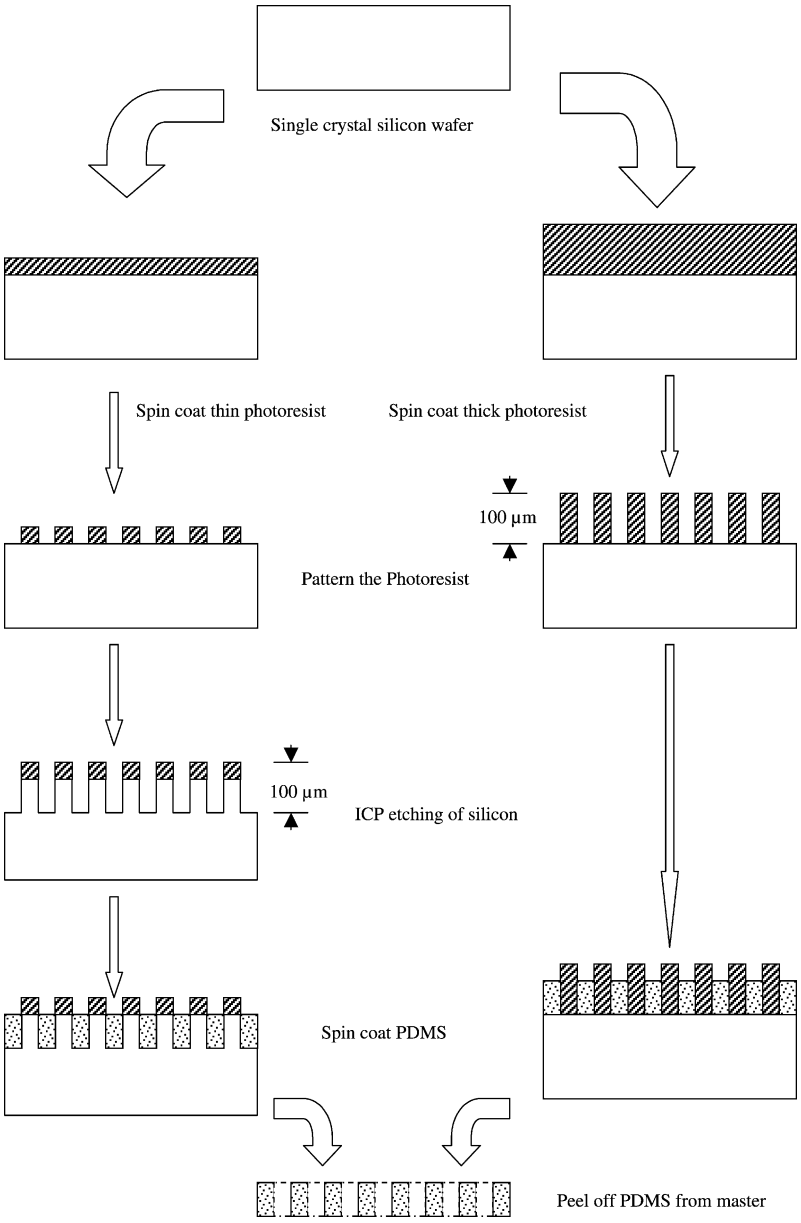

Fig. 4. Schematic illustration of fabrication process for PDMS shadow mask using two different routes.

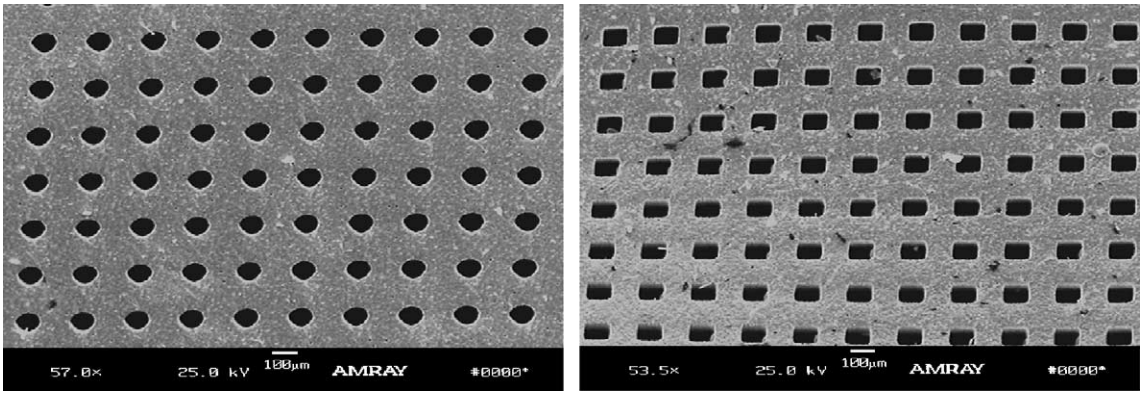

Fig. 5. Scanning electron micrograph (SEM) images of 100 μm squares and circles formed in 70 μm thick PDMS membrane to use it as a shadow mask for electrode deposition.

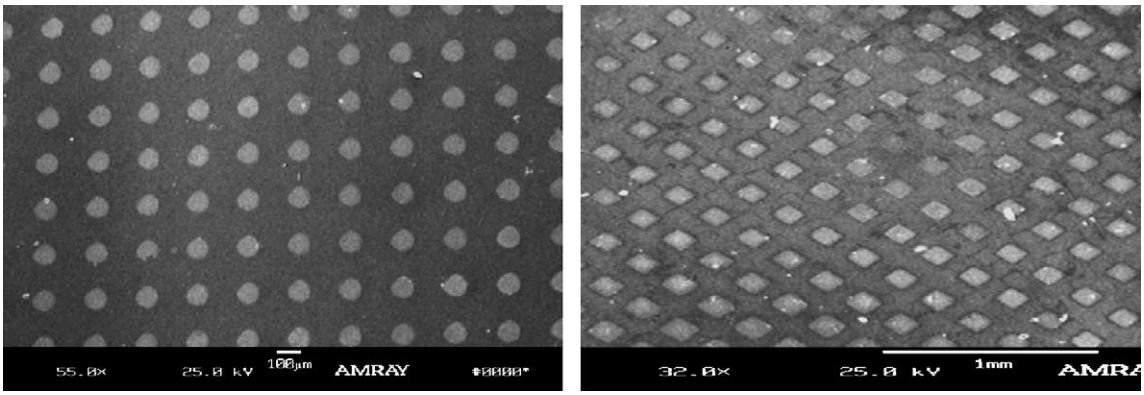

Fig. 6. SEM Images of Ag electrodes on Pt- and Pd-deposited Nafion membrane. Five hundred nanometer of Ag was deposited using PDMS shadow masks which has arrays of 100 μm isolated square and circular holes.

membrane. The membrane was removed from the chamber after depositing catalyst on one side. The Nafion membrane was then flipped and the PDMS shadow mask was placed on it by aligning it with the previously deposited pattern, which was visible through the transparent membrane. Pt was deposited again on the back side in the same manner. After depositing catalyst on both sides of the membrane, 500 nm of silver (Ag) was deposited on both sides as electrodes using the respective PDMS shadow mask. Fig. 6 shows SEM images of sputter-deposited Ag on both sides of the Pt- and Pd-deposited Nafion membranes.

3.4. Novel patterning of electrodes on Nafion membrane by photolithography and lift-off

There are limitations on the features that can be produced in the PDMS shadow mask, and subsequently on the substrate. The features must be discrete and relatively simple in design. Highly elongated patterns (pattern length much greater than pattern width) are not possible as the polymer membrane must be continuous and mechanically stable. In addition, the size of the features that can be produced in the PDMS membrane is restricted. In order to address these limitations, the direct patterning of electrodes on Nafion membrane was also performed by photolithography and lift-off techniques with positive photoresist in order to produce electrically continuous electrode patterns.

The poor adhesion of photoresist to Nafion is a major challenge to direct patterning. We tried thick, viscous photoresist (AZ-9260) for improving adhesion with the membrane. Since the Nafion membrane cannot be heated above 100 °C without causing structural changes to the polymer, modifications were made to the normal photoresist processing parameters. The pretreated Nafion membrane was cut into 4 in. diameter wafer size and blown with nitrogen to dry it thoroughly. The dried membrane was smoothly attached to a PDMS-coated silicon wafer for all subsequent processing steps. The membrane adhered well to PDMS and remained firmly on the wafer even during spin-coating steps. Before spinning, hexamethyldisilazane (HMDS) was coated on the membrane in order to improve photoresist adhesion. Photoresist AZ-9260 was then spin-coated to give a thickness of 10 μm on the Nafion, then soft baked at 70 °C for 5 min. The resist-coated membrane was then exposed with the electrode pattern photomask for 120 s on a standard aligner in proximity mode. Finally, the patterns were developed in an AZ-400 K developer solution (diluted with water in 1:4 ratio) for 60 s. Patterning by photolithography resulted in well-defined photoresist areas on the membrane. Fig. 7 shows SEM images of lithographically defined

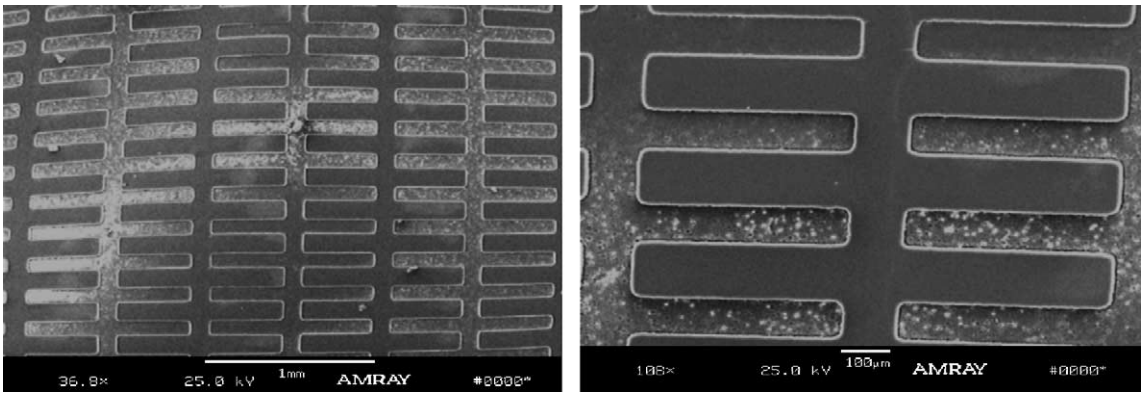

Fig. 7. SEM images of photoresist patterns on Nafion membrane.

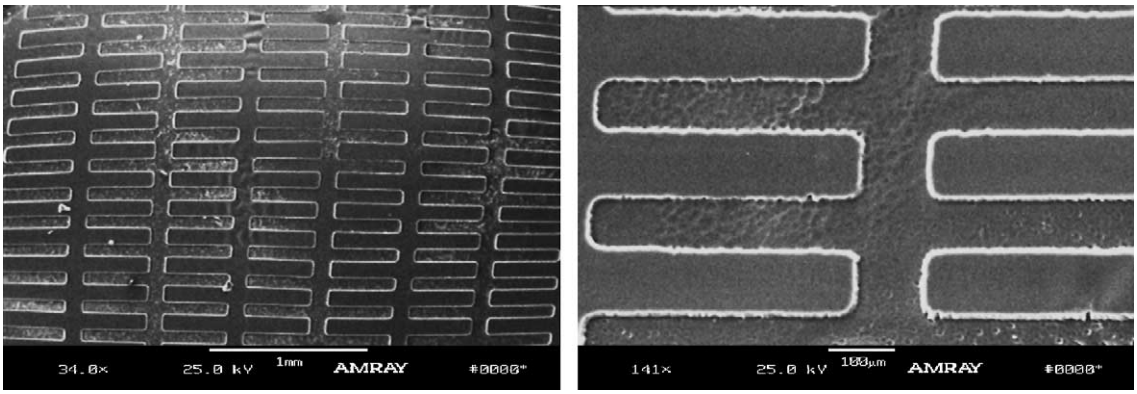

Fig. 8. SEM images of 500 nm thick Ag deposited on patterned Nafion membrane.

patterns on the membrane at different magnifications. Photoresist residues left behind on the membrane after the lithography step can be seen as white spots in the SEM image.

The Nafion membrane wrinkled and formed ridges in acetone, therefore immersion in developer was used for metal lift-off. Prior to metal deposition, the patterned membrane was flood exposed for 120 s to render the resist soluble in developer during the subsequent lift-off step.

It was observed that the adhesion of sputter-deposited silver to the Nafion membrane was poor. In order to improve adhesion, a 5 nm thick titanium layer was sputter-deposited on the membrane before the 500 nm silver layer. Fig. 8 shows SEM images of the Ag-deposited membrane.

After depositing Ti and Ag, the membrane was placed again in the developer solution, which dissolved the previously exposed photoresist. Thus, metals were removed by lift-off from the resist-covered areas of the membrane, giving selective deposition of metals as electrodes on the Nafion membrane. Fig. 9 shows a SEM image of Ti/Ag electrodes on the Nafion membrane after the lift-off step.

Once Ti/Ag was defined as an electrode on membrane, 5 nm of Pt was deposited as a catalyst using the respective PDMS shadow mask.

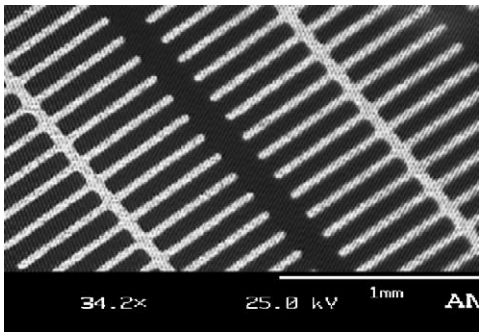

Fig. 9. SEM image of Ag electrodes on Nafion membrane after lift-off.

3.5. Electrical connections and bonding of Nafion membrane to base substrates

The membrane was cut to the base substrate size in length. However, in the perpendicular direction it was kept free standing along one edge in order to provide electrical connections. A 0.5 cm × 0.5 cm pad was provided for electrical connections on the free standing portion of the membrane. Electrical connections were created on both sides by bonding thin wires on the pads with a two component conductive silver epoxy. Epoxy was also used to bond the Nafion membrane to the base substrate. The epoxy was applied on the edges of the base substrate and the Nafion membrane was located on it so that the sputtered area on the membrane was placed in contact with the channel area of the substrate. The membrane–microreactor assembly was then placed on a hot plate until the epoxy hardened. A thin layer of liquid PDMS was then applied to the edges of this assembly and allowed to cure, which helped to prevent gas leakage around the periphery of the final device.

In the case of the PDMS fuel cell, a liquid prepolymer of PDMS was applied to the edges of the PDMS base substrate, and the catalyst and electrode-deposited membrane was then placed on this substrate. The assembly was pressurized and placed on a hot plate for curing at a temperature of 70 °C. This gave a good seal between the base substrate and the membrane.

4. Fuel cell characterization

4.1. Test set-up

A custom-built microreactor test fixture was used to test the micro fuel cell. The test setup consisted of a mounting block, which supported the fuel cell and allowed the introduction and elimination of gases. Temperature control was achieved with a cartridge heater inside the block and a thermocouple in order to monitor and control the temperature. Pure hydrogen was fed to the fuel cell from the cylinder at a

measured flow rate using an electronic mass flow controller, while the cathode side was kept open to atmosphere to draw oxygen from air. The flow of gases and temperatures were automatically monitored and controlled by interfacing the setup with a computer using LabView software.

Open circuit voltage (OCV) was measured by connecting the anode and cathode of the fuel cell directly to a digital multimeter. Current-voltage characteristics were measured using two digital multimeters and a variable load resistor. The generated current was passed through various loads and the cell voltage was recorded as a function of current once the steady state was achieved. The polarization curve measurements were made at temperatures ranging from ambient temperature to 80 °C. The oxidation reaction of hydrogen was characterized by measuring the composition of the product gases. A quadrupole mass spectrometer (QMS) was used to monitor the outlet product composition.

5. Results and discussion

Open circuit voltage and current–voltage characteristics were measured at different temperatures, ranging from room temperature to 80 °C. Also, the effects of hydrogen flow rates and humidification of the hydrogen stream were investigated. Fuel cell performances were measured for different catalyst loadings. The best results were obtained with very thin catalyst (5 nm Pt, which amounts to a Pt loading of 0.014 mg/cm^2) and thicker electrodes (500 nm Ag). The maximum open circuit voltage measured was 840 mV, while the highest current density was 1.90 mA/cm^2 at room temperature conditions. The area of the membrane exposed to gas contact was 0.8 cm^2 while the hydrogen flow rate was 1.0 sccm. The maximum power obtained was 0.375 mW/cm^2 at 0.380 V. Fig. 10 shows *V–I* characteristics obtained from fuel cell while Fig. 11 shows the power drawn from the cell versus current density.

The Nafion membrane patterned by the lithography and lift-off approach to define thicker electrodes and thinner catalyst layers showed almost identical performance.

The power density obtained from these cells based on geometric surface area was low compared to values reported up to 65 mW/cm^2 from the Pt/Nafion PEM fuel cell at a Pt loading of 0.014 mg/cm^2 [23]. From the results it can be inferred that the scale-down problems were associated more with catalyst layers than with gas flow channels. Low current obtained from these cells reflected a small active catalyst area compared to the geometric area of the cell. In addition, direct sputter deposition of catalyst on the membrane has been reported to result in a reduced cell performance [23,29]. Current densities as low as 5 mA/cm^2 were reported for sputter-deposition directly on the Nafion membrane which compares well with our results.

It is established that at a thickness of 5 nm, sputtered Pt forms continuous film on the surface of the Nafion membrane [30]. The sputter deposition therefore resulted in a flat catalyst layer with low porosity and provided only limited

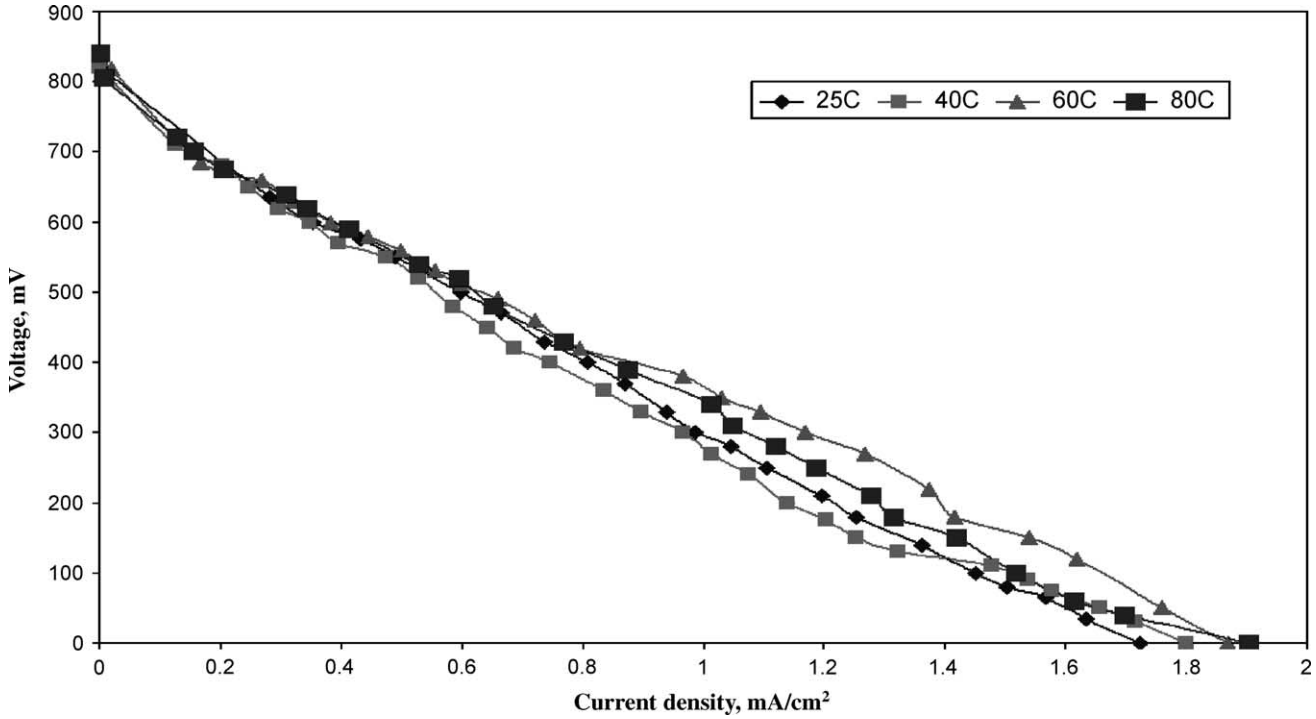

Fig. 10. Current–voltage characteristics of a micro fuel cell with 5 nm thick Pt catalyst and 500 nm thick Ag electrodes.

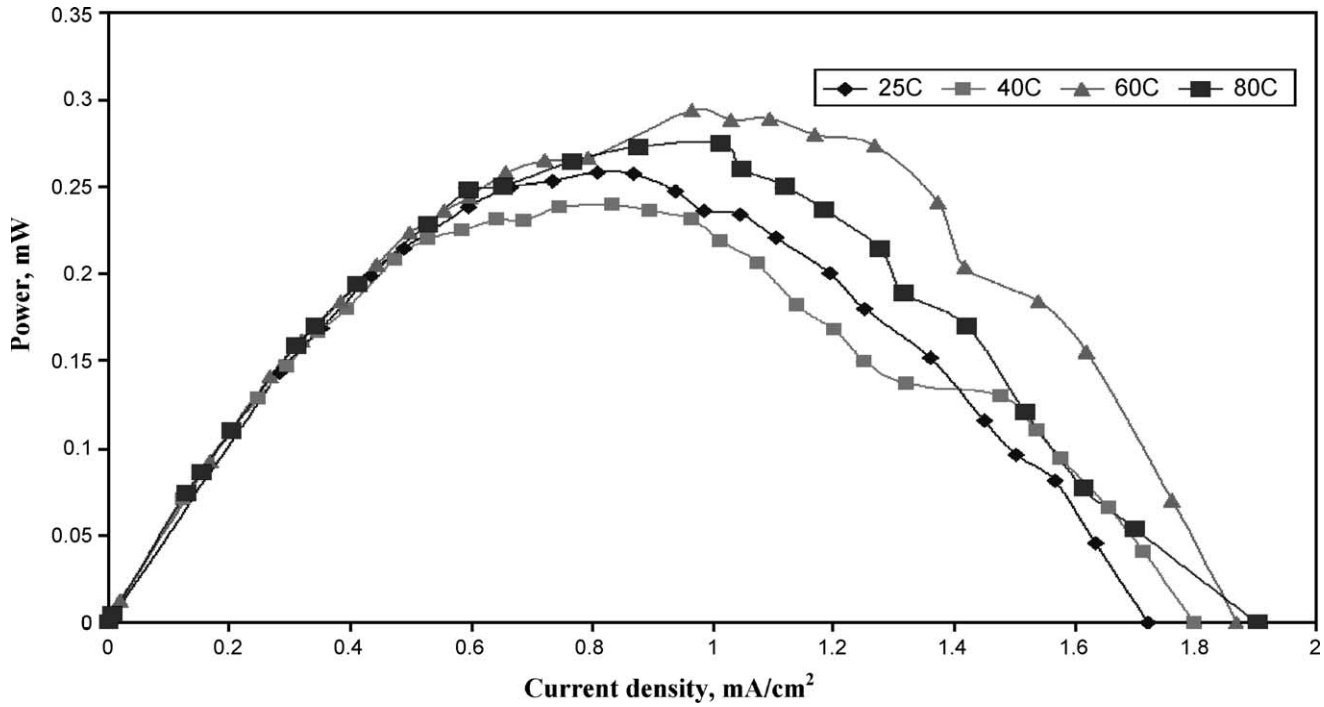

Fig. 11. Power obtained vs. current density at different temperatures from micro fuel cell with 5 nm thick Pt catalyst and 500 nm thick Ag electrodes.

regions where the three phase interface of electrolyte, catalyst, and reactant gas could occur. This interaction is felt to be necessary to enhance both electron and proton conduction [1,2].

During operation of the cell, the membrane, in absence of proper structural support, contracted and formed ridges, which significantly reduced the effective catalyst–gas contact area and lifted the membrane away from the base substrate. To a lesser extent, hydrogen leaks around the periphery of the membrane–base substrate assembly may have limited the pressure drop across the membrane, which in turn limited proton flux through membrane.

Other possible explanations for lower than expected current densities include inadequate active site density of sputtered catalyst films, non-optimal series resistances, use of atmospheric pressure air at the cathode (rather than pressurized oxygen), and poor hydrogen distribution in the microchannels at low flow rates.

In order to gain information about the active catalyst surface area and the utilization of catalyst, it is necessary to characterize the thin layer of sputter-deposited catalyst via physisorption (for accessible surface area) and chemisorption (for active site density). These measurements remain as future work.

Ultimately, porous catalyst and electrode structures are necessary for improving the fuel cell performance. Novel electrode and catalyst design and deposition approaches are necessary to achieve acceptable power densities from micro fuel cells, and they must be compatible with the silicon fabrication processes.

6. Conclusion

Simple and flexible functioning micro fuel cells were produced using a variety of novel microfabrication techniques. Approaches like electrode and catalyst deposition using elastomeric shadow masks and direct patterning on Nafion membrane were investigated for selective deposition. These methods showed promise and allowed novel electrode and catalyst configurations on the membrane surface. The electrodes patterned using the above methods complemented well the thin catalyst layers. The electrodes helped minimize the catalyst loadings, series and contact resistances and at the same time allowed sufficient open surface for reactant gas to access the active catalyst sites.

References

[1] A. Appleby, F. Foulkes, Fuel Cell Handbook, Van Nostrand Reinhold, New York, 1989.
[2] Fuel Cell Handbook, fifth ed., Report prepared by EG&G Services for the US Department of Energy, National Energy Laboratory, October 2000.
[3] C.K. Dyer, J. Power Sources 106 (2002) 31–34.
[4] C. Muller, M. Muller, C. Hebling, Microreactors for energy generation and storage, AIChE (2000).
[5] L. Mex, N. Ponath, J. Muller, Fuel Cells Bull. 4 (39) (2001) 9–12.
[6] J.P. Meyers, M. Helen, J. Power Sources 109 (2002) 76–88.
[7] J. Morse, A.F. Jankowski, R.T. Graff, J. Hayes, J. Vac. Sci. Technol. A 18 (4) (2000) 2003–2005.
[8] W.Y. Sim, G.Y. Kim, S.S. Yang, in: Proceedings of the IEEE Micro Electro Mechanical Systems (MEMS), 2001, pp. 341–344.

[9] H.L. Maynard, J.P. Meyers, J. Vac. Sci. Technol. B Microelectron. Nanometer Struct. 20 (4) (2002) 1287–1297.
[10] H. Chang, P. Koschany, C. Lim, J. Kim, J. New Mater. Electrochem. Soc. 3 (2000) 55–59.
[11] R.S. Besser, X. Ouyang, H. Surangalikar, Chem. Eng. Sci. 58 (2003) 19–26.
[12] H. Suranglikar, R.S. Besser, in: Proceedings of the 6th International Conference on Microreaction Technology (IMRET VI), American Institute of Chemical Engineers, New Orleans, LA, 2002, pp. 248–253.
[13] H. Surangalikar, X. Ouyang, R.S. Besser, Chem. Eng. J. 93 (3) (2003) 217–224.
[14] R.S. Besser, W.C. Shin, J. Vac. Sci. Technol. B 21 (2) (2003) 781–784.
[15] Y. Xia, G.M. Whitesides, Annu. Rev. Mater. Sci. 28 (1998) 153–184.
[16] E.J. Taylor, E.B. Anderson, N.K. Vilambi, J. Electrochem. Soc. 139 (5) (1992) L45–L46.
[17] E.B. Easton, Z. Qi, A. Kaufmann, Electrochem. Solid-State Lett. 4 (5) (2001) A59–A61.
[18] C. Marr, X. Li, J. Power Source 77 (1999) 17–27.
[19] Y.-G. Chun, C.-S. Kim, J. Power Sources 71 (1998) 174–178.
[20] M.S. Wilson, S. Gottesfeld, J. Electrochem. Soc. 139 (1992) L28–L30.
[21] Y.-G. Chun, D.H. Peck, C.S. Kim, D.R. Shin, J. New Mater. Electrochem. Soc. 4 (2001) 31–35.
[22] M.S. Wilson, S. Gottesfeld, J. Appl. Electrochem. 22 (1) (1992) 1–7.
[23] A. Haug, R. White, J. Weidner, W. Haug, S. Shi, J. Electrochem. Soc. 149 (3) (2002) A280–A287.
[24] J.L. Kern, W. Vossen, Thin film processes, vol. II, Academic Press, Boston, MA, 1997, pp. 177–207.
[25] S.J. Lee, S.W. Cha, Y.C. Liu, R. O'Hayre, F.B. Prinz, High power-density polymer-electrolyte fuel cells by microfabrication, in: Proceedings of the Conference on Micro Power Sources, The Electrochemical Society Proceeding Series, vol. 3, Pennington, NJ, 2000.
[26] A.F. Jankowski, J.P. Hayes, R.T. Graff, J.D. Morse, Micro-fabricated thin-film fuel cells for portable power requirements, in: Materials for Energy Storage, generation, and Transport, Materials, The Materials Research Society Symposium Proceeding Series, vol. 730, 2002.
[27] R. Jackman, D. Duffy, O. Cherniavskaya, G. Whitesides, Langmuir 15 (1999) 2973–2984.
[28] D.C. Duffy, J.C. McDonald, O.J. Schueller, G.M. Whitesides, Anal. Chem. 70 (1998) 4974–4984.
[29] S.J. Lee, S.W. Cha, R. O'Hayre, A. Chang-Chien, F.B. Prinz, Miniature Fuel Cells with Non-Planar Interface by Microfabrication, in: Proceedings of Power Sources for New Millennium Conference, The Electrochemical Society Proceeding Series, vol. 22, Pennington, NJ, 2000.
[30] R. O'Hayre, S.-J. Lee, S.-W. Cha, F.B. Prinz, J. Power Sources 109 (2002) 483–493.